AIAA 80-1018R

Closed-Form Solution of Mode Propagation in a Nonuniform Circular Duct

Y. C. Cho*
NASA Lewis Research Center, Cleveland, Ohio
and
K. U. Ingard†
Massachusetts Institute of Technology, Cambridge, Mass.

This paper presents an analytical investigation of higher order mode propagation in a nonuniform circular duct without mean flow. An approximate wave equation is derived on the assumptions that the duct cross section varies slowly and that mode conversion is negligible. Closed-form solutions are obtained for a particular class of converging-diverging circular duct which is here referred to as "*circular cosh duct.*" Numerical results are presented in terms of the transmission loss for the various duct shapes and frequencies. The results are applicable to studies of multimodal propagation as well as single-mode propagation. The results are also applicable to studies of sound radiation from certain types of contoured inlet ducts, or of sound propagation in a converging-diverging duct of somewhat different shape from a cosh duct.

Nomenclature

a = effective length of converging-diverging section of duct
b_0 = duct radius at throat ($x=0$)
$b(x)$ = duct radius
b_-, b_+ = constant radius of left- and right-hand side uniform duct element, respectively
c = sound speed
F = hypergeometric function
J_m = Bessel function of first kind of order m
k = free-space wave constant, ω/c
k_-, k_+ = propagation constant of a mode in left- and right-hand side uniform duct element, respectively
m = circumferential mode number or separation constant
N = normalization constant, see Eq. (22)
n = integer used as radial mode number
q = dimensionless parameter, see Eq. (19)
R = power reflection coefficient
r = radial variable in spherical coordinate system
T = power transmission coefficient
t = time variable
TL = transmission loss, dB
V_0 = dimensionless parameter, see Eq. (19)
x = axial coordinate, see Fig. 1
α = separation constant or eigenvalue
α_{mn} = eigenvalue, nth zero of $J'_m(\alpha)$
β = contraction ratio, b_-/b_0
Γ = gamma function
γ = cutoff ratio of mode referenced to inlet kb_-/α
ζ = dimensionless frequency parameter, $kb_0(1-\beta/\gamma)$
η = normalized variable, see Eqs. (9)
θ = polar angle in local spherical coordinate system, see Fig. 3
$\theta_0(x)$ = half-cone angle corresponding to a duct segment, see Fig. 3
μ = asymmetry parameter, $\frac{1}{4}\ln\{(\beta^2-1/\tau^2)/(\beta^2-1)\}$
ν = converging-diverging section length parameter, a/b_-
ξ = dimensionless axial coordinate variable, see Eq. (19)
ρ = radial variable in cylindrical coordinate system
σ = constant parameter, see Eq. (20) and the following paragraph
τ = ratio between inlet and exit radii, b_+/b_-
Φ = function, see Eq. (17)
φ = azimuthal angle around duct axis
Ψ = acoustic velocity potential
ω = angular frequency

Presented as Paper 80-1018 at the AIAA 6th Aeroacoustics Conference, Hartford, Conn., June 4-6, 1980; submitted July 21, 1980; revision received July 20, 1981. This paper is declared a work of the U. S. Government and therefore is in the public domain.

*Aerospace Engineer. Member AIAA.
†Professor of Physics and of Aeronautics and Astronautics.

I. Introduction

ONE of the unique features of the noise field produced by axial flow fans or compressors is the dominance of spinning modes in the fan duct. An additional feature in aircraft applications is that the cross section of a fan duct varies along the duct axis. Consequently, in order to understand the overall acoustic characteristics of a fan duct system, it is imperative to examine the propagation of spinning modes (or higher order modes) in nonuniform ducts.

The higher order mode propagation in nonuniform ducts has been previously investigated by a number of authors. The widely used methods are numerical methods,[1-3] semi-numerical methods,[4] various perturbation methods such as the WKB method or multiple-scale variable methods,[5] and the Born approximation.[6] One of the drawbacks of numerical methods is the failure to provide compact expressions for the various quantities of interest and a corresponding lack of physical insight into the problem. Furthermore, in numerical methods the boundary conditions are satisfied only approximately and the resulting error is not always easy to assess. Perturbation methods have been used to find approximate solutions, but they still require extensive computation to yield numerical results for quantities of practical interest, such as the transmission coefficients. Furthermore, most approximations used thus far have been limited to first-order perturbations with related limitations in the range of the validity of the results, such as the limitation that the relative constriction be small. Also, it should be mentioned that the first-order perturbations predict no attenuation above the cutoff frequency at the throat. Although an extension to higher order perturbations can be made formally, it is quite cumbersome to carry out and it has rarely been done.

In this paper, we develop a new approach with fewer limitations. The basic idea involved is to recognize that higher

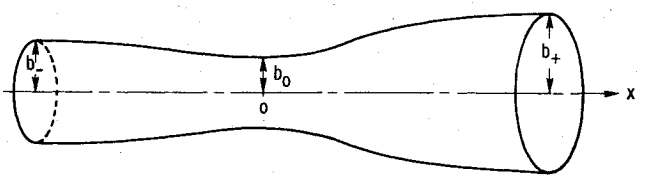

Fig. 1 Circular cosh duct ($\beta=\nu=\tau=1.5$).

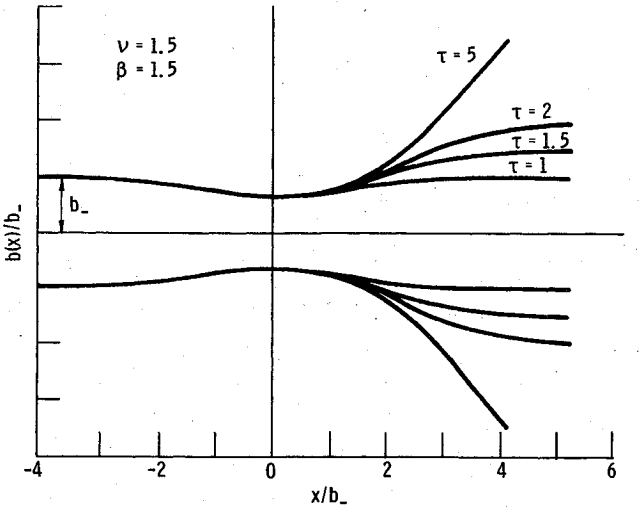

Fig. 2 Various shapes of circular cosh duct.

order mode propagation in a nonuniform duct is analogous to problems in quantum mechanics dealing with matter wave propagation in a system with spatially varying potential energy. In the latter case, exact solutions are known for certain barrier types of potential.[7] These solutions are used here to solve the acoustic problem for a class of converging-diverging circular ducts, which are equivalent to the potential barriers. The duct shapes can be varied by means of three independent duct parameters, and cover a wide range of ducts of practical interest. The final results include wave functions and transmission and reflection coefficients, all in a closed form.

II. Circular Cosh Duct

The typical nonuniform circular duct under consideration, which will be referred to as "*circular cosh duct*" is composed of two asymptotically uniform circular duct elements which are smoothly coupled through a converging-diverging section, as illustrated in Fig. 1. The shape is completely determined in terms of the radius $b(x)$ which is given by

$$\left(\frac{b_-}{b(x)}\right)^2=\beta^2-(\beta^2-1)e^{2\mu}\cosh(2\mu)+(\beta^2-1)e^{2\mu}$$
$$\times\left[\cosh^2\mu\,\mathrm{sech}^2\left(\frac{x-\mu a}{a}\right)-\sinh(2\mu)\tanh\left(\frac{x-\mu a}{a}\right)\right] \quad (1a)$$

where the parameters are defined in the Nomenclature. For a symmetric circular cosh duct ($\tau=1$, $\mu=0$), this equation reduces to

$$\left(\frac{b_-}{b(x)}\right)^2=1+(\beta^2-1)\,\mathrm{sech}^2\left(\frac{x}{a}\right) \quad (1b)$$

The duct shape given by Eq. (1a) can be adjusted by means of the three dimensionless parameters β, ν, and τ, allowing one to vary 1) the contraction ratio β, 2) the effective length of the converging-diverging section ν, and 3) the ratio between the inlet and exit radii τ. Equation (1a) should cover a wide range of converging-diverging circular ducts of practical interest. Various circular cosh duct shapes with fixed β and ν are displayed in Fig. 2.

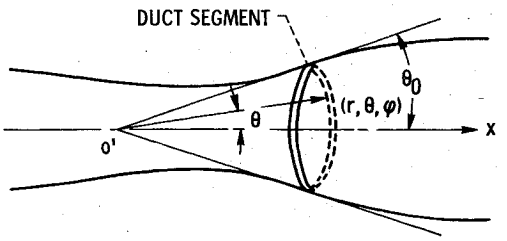

Fig. 3 Duct segment and local spherical coordinate system.

It should be mentioned here that the results of the present investigation can be used to study the acoustic characteristics of a variety of converging-diverging ducts with slowly varying cross sections, which may slightly differ in shape from the circular cosh ducts. The supporting argument for this statement is as follows: The frequency range where our understanding of the acoustic properties of converging-diverging ducts is lacking is near the cutoff frequency of a relevant duct mode. In this frequency range, the axial variation of wave phase is slow, and the propagation characteristics are hardly affected by comparatively small-scale changes of the duct shape as long as the cross section varies slowly.

III. Wave Equation in a Nonuniform Circular Duct

In this section, a horn equation will be derived for higher order mode propagation in a nonuniform circular duct under the following assumptions: 1) the slope b' of the duct wall remains small, and 2) the mode conversion (from one mode to another) is negligible. In addition, modes for such a nonuniform circular duct will be defined.

The equation is derived first for a small segment of the duct using *locally suitable spherical coordinates* and is then transformed into a form which involves the duct parameters and the axial coordinate x. Let us consider a small segment of the duct and local spherical coordinates (r, θ, φ) as illustrated in Fig. 3. The duct segment is so short that it may be regarded as conical, that is, b' hardly changes within the duct segment. The origin of the spherical coordinate system is chosen somewhere on the axis such that a coordinate surface $\theta=\theta_0$ (cone) tangentially contacts the wall of the duct segment. The half-cone angle θ_0 is equal to b' to second-order approximation.

With the assumption of harmonic time dependence $e^{-i\omega t}$ the wave equation for spherical coordinates is

$$\frac{1}{r^2}\left[\frac{\partial}{\partial r}\left(r^2\frac{\partial\Psi}{\partial r}\right)+\frac{1}{\sin\theta}\frac{\partial}{\partial\theta}\left(\sin\theta\frac{\partial\Psi}{\partial\theta}\right)\right.$$
$$\left.+\frac{1}{\sin^2\theta}\frac{\partial^2\Psi}{\partial\varphi^2}\right]+k^2\Psi=0 \quad (2)$$

where Ψ is the acoustic velocity potential and $k=\omega/c$. With the substitution

$$\Psi=H(r)\,Y(\theta)\,Q(\varphi) \quad (3)$$

Eq. (2) is separated as follows:

$$\frac{d^2H}{dr^2}+\frac{2}{r}\frac{dH}{dr}+\left[k^2+\left(\frac{\alpha}{r\theta_0}\right)^2\right]H=0 \quad (4)$$

$$\frac{1}{\sin\theta}\frac{d}{d\theta}\left(\sin\theta\frac{dY}{d\theta}\right)+\left[\left(\frac{\alpha}{\theta_0}\right)^2-\left(\frac{m}{\sin\theta}\right)^2\right]Y=0 \quad (5)$$

$$d^2Q/d\varphi^2 + m^2Q = 0 \tag{6}$$

Here α and m are the separation constants and θ_0 has been inserted for convenience.

We consider Eq. (6) first, the solution to which is

$$Q = e^{im\varphi} \tag{7}$$

Here m must be an integer for Q to be a single-valued function, and it is known as the circumferential mode number. It is obvious that this solution is valid throughout the duct as long as the cylindrical symmetry is maintained.

Equation (5) is an equation for the associated Legendre functions. These are not, however, convenient for the present problem. The main difficulty arises in determining eigenvalues and in transforming them from the local coordinates to the duct coordinates. Therefore, a simplified form of Eq. (5) will be used here. In the region of interest $0 \le \theta \le \theta_0$, one can replace $\sin\theta$ by θ to the second-order approximation in b'. Equation (5) can then be written as

$$\frac{d^2Y}{d\theta^2} + \frac{1}{\theta}\frac{dY}{d\theta} + \left[\left(\frac{\alpha}{\theta_0}\right)^2 - \left(\frac{m}{\theta}\right)^2\right]Y = 0 \tag{8}$$

This is the Bessel equation.

It is convenient to introduce a normalized variable η defined as

$$\eta = \theta/\theta_0 \tag{9a}$$

where $0 \le \eta \le 1$. Note that, in the limit $\theta_0 \to 0$, the duct segment becomes cylindrical and Eq. (9a) is replaced by

$$\eta = \rho/b \tag{9b}$$

where ρ is the radial coordinate in the cylindrical coordinate system.

With the substitution of Eq. (9a), Eq. (8) is transformed into

$$\frac{d^2Y}{d\eta^2} + \frac{1}{\eta}\frac{dY}{d\eta} + \left[\alpha^2 - \left(\frac{m}{\eta}\right)^2\right]Y = 0 \tag{10}$$

Note that η is not a local coordinate variable and that, unlike Eq. (8), Eq. (10) is valid throughout the duct as long as the assumptions 1 and 2 remain valid. The physically acceptable solution to Eq. (10) is the Bessel function of the first kind. Thus we have

$$Y = J_m(\alpha\eta) \tag{11}$$

From the boundary condition at the duct wall, eigenvalues are determined as follows

$$\alpha = \alpha_{mn}, \quad n = 0,1,2\ldots \tag{12}$$

α_{mn} being the nth zero of $J'_m(\alpha)$.

Corresponding to each combination of m and α_{mn}, the solution is uniquely defined in terms of the product

$$e^{im\varphi}J_m(\alpha_{mn}\eta)$$

This eigenfunction is defined throughout the duct, η being given by Eq. (9a) for a conical segment or by Eq. (9b) for a cylindrical segment. Consequently, a mode, which is in one-to-one correspondence with an eigenfunction, has been defined for a nonuniform duct.

We now return to Eq. (4). This equation, when transformed to the duct coordinates, is the one which governs propagation of a mode in the duct. The necessary transformation is accomplished by replacing the local coordinate r with the duct parameters and the axial coordinate x. To this end, we use the following relations:

$$\theta_0 \cong b' \tag{13}$$

$$d/dr \cong d/dx \tag{14}$$

$$r \cong b/b' \tag{15}$$

These equations are valid for a point within the duct segment and are accurate to the order of $(b')^2$.

On inserting Eqs. (13-15) into Eq. (4), we obtain

$$\frac{d^2H}{dx^2} + \frac{2b'}{b}\frac{dH}{dx} + \left[k^2 - \left(\frac{\alpha}{b}\right)^2\right]H = 0 \tag{16}$$

This is the equation for higher order mode propagation in a nonuniform circular duct. Its solutions will be sought in the following section.

IV. Higher Order Mode Propagation in a Circular Cosh Duct

In this section, we seek solutions to Eq. (16) for the circular cosh ducts described in Sec. II.

It is convenient to introduce a new function $\Phi(x)$, which is defined by

$$H(x) = \Phi(x)/b(x) \tag{17}$$

On inserting this into Eq. (16), we obtain

$$\frac{d^2\Phi}{dx^2} + \left[k^2 - \left(\frac{\alpha}{b}\right)^2\right]\Phi = 0 \tag{18}$$

where bb''/α^2 has been discarded on the assumption that it is negligible compared with unity. It can be readily shown that this equation is also valid for the fundamental mode propagation ($\alpha = 0$).

Equation (18) is similar, in form, to the one-dimensional Schroedinger equation, with k^2 and $(\alpha/b)^2$ corresponding to the total energy and the potential energy, respectively.[7] With the substitution of Eq. (1a), Eq. (18) is written as

$$\frac{d^2\Phi}{d\xi^2} + [q^2 - V_0(\cosh^2\mu\ \operatorname{sech}^2\xi - \sinh(2\mu)\tanh\xi)]\Phi = 0 \tag{19}$$

where

$$\xi = (x - \mu a)/a$$

$$q^2 = (ka)^2 + V_0\cosh(2\mu) - (\alpha\beta\nu)^2$$

$$V_0 = e^{2\mu}(\beta^2 - 1)(\alpha\nu)^2$$

Equation (19) can be solved exactly in accordance with the procedure given in Sec. 12.3 of Ref. 7. With the incident wave coming from $x = -\infty$, the solution is given by

$$\Phi = Ne^{(i/2)(k_+ - k_-)a\xi}(2\cosh\xi)^{(i/2)(k_+ + k_-)a}$$

$$\times F\left(\frac{1}{2} - \frac{i}{2}(k_+a + k_-a - \sigma),\ \frac{1}{2} - \frac{i}{2}(k_+a + k_-a + \sigma),\right.$$

$$\left. 1 - ik_+a;\ \frac{1}{e^{2\xi} + 1}\right) \tag{20}$$

Here F is the hypergeometric function, N a constant to be determined, and

$$k_\pm = \sqrt{k^2 - (\alpha/b_\pm)^2} \qquad \sigma = \sqrt{4V_0\cosh^2\mu - 1}$$

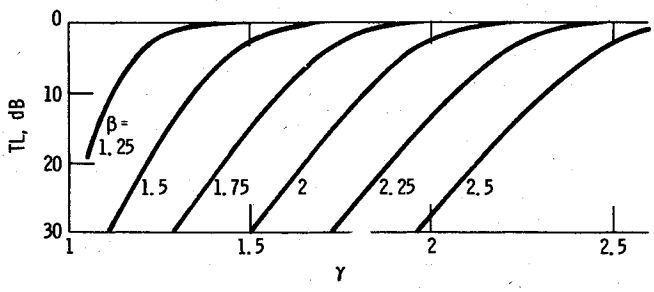

Fig. 4 Power transmission loss of (1,0) mode vs frequency parameter for various values of β, with $\nu = \tau = 1$.

This solution, ξ being replaced by x, can be written asymptotically at $x = \pm\infty$ as follows

$$\Phi \xrightarrow{x\to-\infty} Ne^{-ik_+\mu a}e^{ik_+x} \tag{21a}$$

$$\Phi \xrightarrow{x\to-\infty} \frac{N\Gamma(1-ik_+a)\Gamma(-ik_-a)e^{-ik_-\mu a}e^{ik_-x}}{\Gamma\left(\frac{1}{2}-\frac{i}{2}(k_+a+k_-a+\sigma)\right)\Gamma\left(\frac{1}{2}-\frac{i}{2}(k_+a+k_-a-\sigma)\right)}$$

$$+\frac{N\Gamma(1-ik_+a)\Gamma(ik_-a)e^{ik_-\mu a}e^{-ik_-x}}{\Gamma\left(\frac{1}{2}-\frac{i}{2}(k_+a-k_-a+\sigma)\right)\Gamma\left(\frac{1}{2}-\frac{i}{2}(k_+a-k_-a-\sigma)\right)} \tag{21b}$$

where Γ is the gamma function. The asymptotic solution in Eq. (21a) corresponds to the transmitted wave and the first and second terms of Eq. (21b) correspond to the incident and the reflected waves, respectively. Requiring the incident wave to have unit amplitude, we have

$$N=\frac{b_-\Gamma\left(\frac{1}{2}-\frac{i}{2}(k_+a+k_-a+\sigma)\right)\Gamma\left(\frac{1}{2}-\frac{i}{2}(k_+a+k_-a-\sigma)\right)}{\Gamma(1-ik_+a)\Gamma(-ik_-a)e^{-ik_-\mu a}} \tag{22}$$

The solution in Eqs. (20) and (17) and the corresponding eigenfunction will give the complete solution in the circular cosh duct. For the incident wave given by

$$\Psi_I = e^{im\varphi}J_m(\alpha_{mn}\eta)e^{ik_-x}, \text{ at } x=-\infty \tag{23}$$

the resultant wave in the duct is

$$\Psi = Ne^{im\varphi}J_m(\alpha_{mn}\eta)\frac{1}{b}e^{(i/2)(k_+-k_-)(x-\mu a)} \times [e^{x/a-\mu}+e^{-[x/a-\mu]}]^{(i/2)(k_++k_-)a} \times F\left(\frac{1}{2}-\frac{i}{2}(k_+a+k_-a-\sigma),\ \frac{1}{2}-\frac{i}{2}(k_+a+k_-a+\sigma),\ \times 1-ik_+a;\ \frac{1}{e^{2[x/a-\mu]}+1}\right) \tag{24}$$

The reflection and transmission coefficients for the wave amplitude can be readily computed from Eqs. (21a) and (21b). In the case of no mean flow, the reflection and transmission coefficients for the acoustic power are obtained as the absolute squares of the respective amplitude coefficients. In the following discussions, we will use the acoustic power reflection and transmission coefficients, which are given by

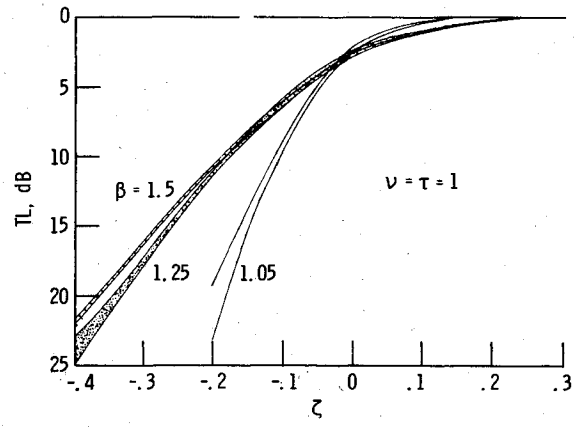

Fig. 5 Transmission loss vs ζ for $\beta = 1.05$, 1.25, and 1.5 for $\nu = \tau = 1$. Each curve (stripe) includes 10 modes ranging from (2,0) to (8,5).

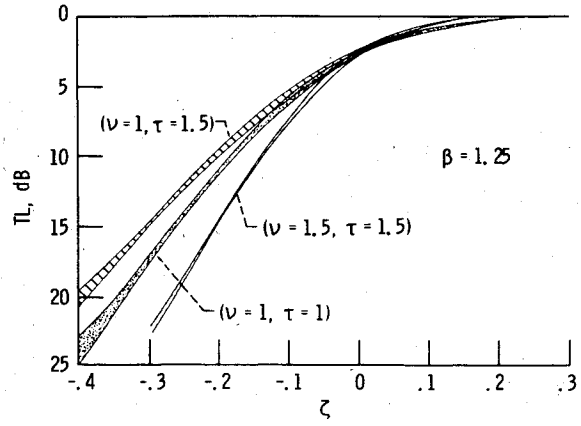

Fig. 6 Transmission loss vs ζ for $\nu = 1$; $\tau = 1$, $\nu = 1.5$; $\tau = 1.5$ with $\beta = 1.25$. Each curve (stripe) includes 10 modes ranging from (2,0) to (8,5).

$$R=\frac{\cosh[\pi a(k_+-k_-)]+\cosh(\pi\sigma)}{\cosh[\pi a(k_++k_-)]+\cosh(\pi\sigma)} \tag{25}$$

$$T=\frac{2\sinh(\pi k_+a)\sinh(\pi k_-a)}{\cosh[\pi a(k_++k_-)]+\cosh(\pi\sigma)} \tag{26}$$

In deriving these equations, we have used the following properties of the Γ function

$$|\Gamma(1+iz)|^2=\frac{\pi z}{\sinh(\pi z)}$$

$$\left|\Gamma\left(\frac{1}{2}+iz\right)\right|^2=\frac{\pi}{\cosh(\pi z)}$$

Note that the results given in Eqs. (25) and (26) satisfy energy conservation, that is

$$R+T=1 \tag{27}$$

V. Numerical Results and Discussions

Some numerical results are presented in Figs. 4-7. Displayed in the figures is the acoustic power transmission loss (TL) for various values of the duct parameters and a frequency parameter (γ or ζ). The TL is defined as

$$\text{TL(dB)} = -10\log_{10}(T) \tag{28}$$

In Fig. 4, the TL of the (1,0) mode is plotted as a function of γ, the cutoff ratio of the mode at the duct inlet, defined as

$$\gamma = kb_{-}/\alpha \tag{29}$$

Note that the value of γ is not less than unity for propagating incident wave mode. The duct parameters included in the figure are various values of β and $\nu = \tau = 1$. As expected, the TL decreases with increasing frequency, in a similar way for different values of β. The rate of TL change ($dTL/d\gamma$) is the greatest in the vicinity of $\gamma = \beta$, which corresponds to the cutoff frequency of the mode at the throat. Note that, at $\gamma = \beta$, the TL is nonzero with a value of about 2.5-3 dB. This result is in contrast to that of the first-order perturbation solutions, which predict no attenuation for $\gamma \geq \beta$.[4,5]

In Figs. 5 and 6, the TL of various modes is plotted as a function of ζ for various values of the duct parameters. Here ζ is a frequency parameter which is defined as

$$\zeta = kb_0[1 - (\beta/\gamma)] \tag{30}$$

Note that β/γ is the inverse of the cutoff ratio at the throat and that $\zeta = 0$ corresponds to the cutoff frequency at the throat.

Each curve (narrow stripe) in these figures includes the TL of 10 randomly selected modes ranging from the (2,0) mode to the (8,5) mode. This shows that the ζ dependence of the TL is almost the same for all the higher order modes. This result is remarkable and is useful, especially for studies of multimodal propagation in a converging-diverging duct. In some cases, one may not need to identify individual modes. An example of such cases can be found in conjunction with a study of multimodal radiation from a uniform duct.[8] The acoustic power distribution vs γ in the duct can often be inferred from the measured radiation pattern. For a known γ distribution of the acoustic power, the present result can be immediately applied to determine the effect of the converging-diverging section on the multimodal propagation. Recall that the parameter ζ contains γ explicitly, not the eigenvalues of modes.

Figure 5 includes calculations for $\beta = 1.05$, 1.25, and 1.5 with $\nu = \tau = 1$. The result shows that, for $\zeta < 0$, the TL is more sensitive to the frequency for the smaller value of β. We also notice that the calculations for different modes collapse better as β increases.

Figure 6 includes calculations for different values of ν and τ, with $\beta = 1.25$, We first compare the curves (narrow stripes) for ($\nu = 1$, $\tau = 1$) and for ($\nu = 1$, $\tau = 1.5$) in order to see the effect of τ. For $\zeta < -0.15$, the TL for $\tau = 1.5$ is smaller than that for $\tau = 1$. This result is due to the fact that the duct segment in which the modes are cut off is shorter for $\tau = 1.5$ than for $\tau = 1$ (see Fig. 2). However, the two curves do not show much difference for $\zeta > -0.15$. This point will be further discussed later with reference to Fig. 7.

We now compare the curves for ($\nu = 1$, $\tau = 1.5$) and for ($\nu = 1.5$, $\tau = 1.5$) in Fig. 6 in order to see the effect of ν. For $\zeta < 0$, the TL is larger for $\nu = 1.5$ than for $\nu = 1$. This result is the direct consequence of the fact that the larger values of ν represent the longer converging-diverging section. The length of the duct segment in which the modes are cut off increases with increasing value of ν.

In Fig. 7, the TL of the (1,0) mode is plotted as a function of τ for the various values of γ, ν, and β. For $\gamma > \beta$, the TL hardly depends on τ. For $\gamma < \beta$, the TL slightly decreases initially with increasing values of τ, and asymptotically reaches a constant value near $\tau = 1.5$. It remains unchanged for further increase of the value of τ. This finding suggests that the results of the present investigation can be used for studies of higher order mode transmission from a contoured inlet duct.

To account for the last statement, we consider a contoured inlet duct as illustrated in Fig. 8. The inlet duct is produced

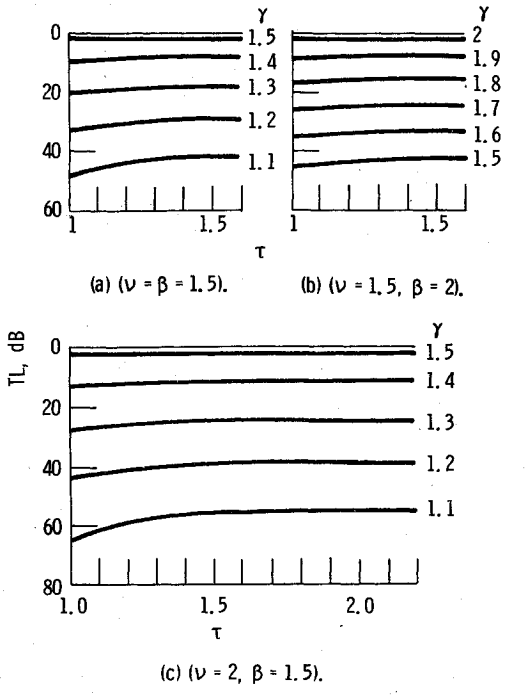

Fig. 7 Power transmission loss of (1,0) mode vs τ.

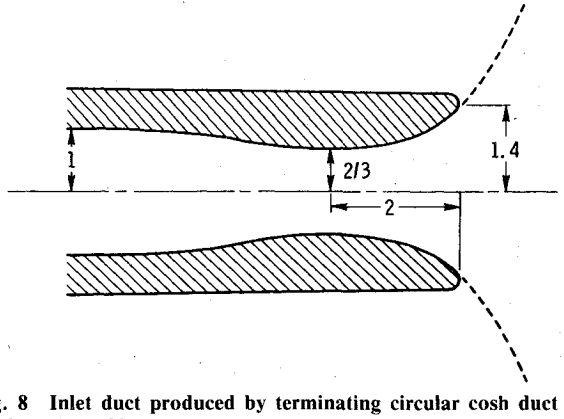

Fig. 8 Inlet duct produced by terminating circular cosh duct with $\nu = \beta = 1.5$, $\tau = 30$.

from a circular cosh duct with a large value of τ. The circular cosh duct is terminated at a distance where the duct radius is $1.4b_{-}$. The cutoff frequency at the termination is smaller than that of the left-hand side uniform duct element by the factor of 1.4. Thus, for a propagating incident wave mode ($\gamma > 1$), the reflection due to the duct termination is negligible.[9] It follows then that the TL for the contoured inlet duct is expected to be the same as that for the full circular cosh duct.

It should probably be mentioned that the slope b' can be fairly large for a large value of τ in a portion of the diverging section. Although it seems to violate the assumptions used in the analysis, the numerical results remain valid. The supporting argument is that, in the first place, the slope remains small within some distance downstream from the turning point where the mode changes from cutoff to cuton. In the second place, the sound attenuation takes place mostly in the duct segment where the mode is cut off, whereas the diverging section, like a loud-speaker horn,[10] helps the unattenuated portion of the sound to be radiated. The radiation efficiency is not sensitive to the slope as long as the duct divergence is smooth and the frequency is not close to the cutoff frequency at the termination.[9] Lastly, even a fairly large slope, e.g., $b' = 1$, is not so large as to invalidate the approximations

made in the analysis. For instance, for $b'=1$, $\theta_0=\pi/4$ and $\sin\theta_0=0.707$; thus, the error involved in replacing $\sin\theta_0$ by θ_0 is about 11%.

VI. Conclusion

In an attempt to improve the understanding of the acoustic characteristics of a fan duct system, we have investigated higher order mode propagation in a particular class of converging-diverging circular duct, called "*the circular cosh duct.*" The duct shape can be adjusted by means of three duct parameters, covering a wide range of converging-diverging ducts of practical interest.

An approximate wave equation has been derived and exact closed-form solutions have been obtained. No mean flow effects have been included. The expressions for the reflection and transmission coefficients of a mode are simple. With an appropriate choice (ζ) of frequency parameter, the results have been shown to be nearly independent of individual modes and can, therefore, be immediately used for studies of multimodal propagation. The results are also applicable to studies of sound radiation from certain types of contoured inlet ducts, or of sound propagation in a converging-diverging duct which differs somewhat from a cosh duct in shape.

References

[1] Alfredson, R. J., "The Propagation of Sound in a Circular Duct of Continuously Varying Cross-Sectional Area," *Journal of Sound and Vibration,* Vol. 23, Aug. 1972, pp. 433-442.

[2] Astley, R. J. and Eversman, W., "A Finite Element Method for Transmission in Nonuniform Ducts Without Flow," *Journal of Sound and Vibration,* Vol. 57, April 1978, pp. 367-388.

[3] Kaiser, J. E. and Nayfeh, A. H., "A Wave Envelop Technique for Wave Propagation in Nonuniform Ducts," AIAA Paper 76-496, July 1976.

[4] Hogge, H. D. and Ritze, E. W., "Theoretical Studies of Sound Emission from Aircraft Ducts," AIAA Paper 73-1012, Oct. 1973.

[5] Neyfeh, A. H. and Telionis, D. P., "Acoustic Propagation in Ducts with Varying Cross Section," *Journal of the Acoustical Society of America,* Vol. 54, Dec. 1973, pp. 1654-1661.

[6] Tam, C. K. W., "Transmission of Spinning Acoustic Modes in a Slightly Non-uniform Duct," *Journal of Sound and Vibration,* Vol. 18, Oct. 1971, pp. 339-351.

[7] Morse, P. M. and Feshbach, H., *Methods of Theoretical Physics,* McGraw-Hill Book Co., New York, 1953, Chap. 12.

[8] Rice, E. J., "Multimodal Far-Field Acoustic Radiation Pattern using Mode Cutoff Ratio," *AIAA Journal,* Vol. 16, Sept. 1978, pp. 906-911.

[9] Cho, Y. C., "Rigorous Solutions for Sound Radiation from Circular Ducts with Hyperbolic Horns or Infinite Plane Baffle," *Journal of Sound and Vibration,* Vol. 69, April 1980, pp. 405-425.

[10] Morse, P. M., *Vibration and Sound,* McGraw-Hill Book Co., New York, 1948.